Internal friction of polycrystalline ceramic oxides

Giuseppe Pezzotti
Department of Materials, Kyoto Institute of Technology, Sakyo-ku, Matsugasaki, 606-8585 Kyoto, Japan
(Received 2 November 1998)

Low-frequency internal friction behavior was investigated in high-purity Al_2O_3 and MgO polycrystals, with emphasis placed on the anelastic peak component arising from grain-boundary relaxation. Internal friction measurements were performed at temperatures up to ≈2000 K, with varying both the oscillation frequency and the grain size of the polycrystal by about one order of magnitude. A fitting procedure is shown which enables us to separate the anelastic peak component from the overall internal friction response. An analysis of the peak shift at frequency change was considered as a method of experimentally deriving both the activation energy for the elementary transport phenomenon occurring with viscous slip at the grain boundary, and the magnitude of the intrinsic grain-boundary viscosity. A classification of the viscous response of grain boundaries according to their degree of coherency and an estimate of their thicknesses, namely the region over which atomic diffusion is enhanced, was also attempted. For this purpose, a peak deconvolution analysis was performed with the evolution of the peak morphology monitored as a function of grain growth in the respective polycrystals when subjected to repeated annealing cycles. [S0163-1829(99)04830-4]

I. INTRODUCTION

The kinetics of many atomic transport phenomena in ceramic oxides such as sintering, grain growth, and creep are controlled by the rate of solid-state diffusion. At present, the elementary mechanisms of lattice diffusion in oxide crystals are reasonably well understood theoretically, and a large body of experimental data is fairly consistent with the theory.[1] Diffusion along grain boundaries has also been thoroughly investigated,[2–4] although several features concerning its elementary mechanisms are not well understood. For example, it was predicted theoretically in early studies that a space charge should exist at all interfaces in ionic materials,[5–7] thus affecting grain-boundary diffusion in ceramic oxides (for a review, see Kingery[8,9]). However, Yan *et al.*[10] have experimentally evaluated such a grain-boundary space charge and concluded that it has only a negligible effect, if any, on the intrinsic grain-boundary diffusivity of high-purity (ionic) ceramic polycrystals.

Another point of uncertainty is the effect of crystal structure and crystallographic misorientation of neighboring grains on the grain-boundary diffusion phenomenon. The enhanced transport observed at the grain boundary is theorized to occur because either the jump frequency of the kind of defects present at grain boundaries is greater than in the lattice, or that the concentration of defects in the boundary is higher than those in the bulk lattice. Both terms together might affect this phenomenon. Wuensch and Vasilos[11] have reviewed the early literature on grain-boundary diffusion in oxides and have concluded that the enhanced diffusion along grain boundaries is only observed when there is evidence of solute segregation or precipitation. However, detailed studies of transport utilizing radioactive tracer atoms in both polycrystals[12] and bicrystals[13] with high-purity characteristics show a strong enhancement of diffusion along grain boundaries compared to bulk lattice. A large degree of anisotropy in the grain-boundary diffusion of MgO was recently found by Osenbach and Stubican[14] as well. This finding indicates that grain-boundary diffusion in a rocksalt cubic structure such as MgO ceramic, should be strongly related to the crystallographic misfit orientation of neighboring grains. Thus, it should display the properties of a dislocation-pipe diffusion mechanism, similar to the grain-boundary diffusion observed in many metallic systems.[15] Crystallographic misfit between adjacent grains is therefore expected to produce even greater influence on the local grain-boundary diffusion in more complicated crystal structures such as hexagonal Al_2O_3 for example.

In an oxide polycrystal, a large variety of grain-boundary types are observed to exist and, with their different inherent characteristics, contribute to the macroscopic diffusion-related properties of the polycrystal. Annealing experiments to produce grain growth should result in significant alterations of the grain-boundary structure. In grain-growth experiments performed on oxide ceramics, however, little quantitative information about the evolution of the grain-boundary structure upon grain growth is available. Both high-resolution microscopy and radioactive tracer experiments possess the necessary atomic resolution to understand the elementary diffusion mechanisms of individual grain boundaries. But, these techniques are not easily manipulable by statistical determinations and usually need extrapolation to explain macroscopic properties. On the other hand, accurate measurements of grain growth or creep characteristics have been recommended as a tool by which to obtain information on diffusion processes in polycrystalline ceramics, particularly those associated with grain boundaries in oxides.[16,17] Despite the precision of those studies, the details of the diffusion behavior are not resolvable into individual grain boundary responses, and the information available through these indirect experimental techniques is only an average.

In this paper, we attempt to use internal friction measurements to characterize the viscous behavior of grain boundaries in polycrystalline ceramic oxides. Free-decay measurements are performed on high-purity Al_2O_3 and MgO

polycrystals, as a function of three independent variables: temperature, frequency, and grain size. These two oxides are thought to provide useful models for two classes of ceramic materials, viz., (1) Al_2O_3, as a hard, strongly anisotropic ceramic; and, (2) MgO, as a somewhat more ductile, cubic material. In particular, it will be shown that an analysis of the temperature and frequency dependence of the anelastic component (i.e., the grain-boundary peak component[18,19]) of internal friction provide a method of determining the inherent (average) viscosity (i.e., diffusivity) of the ceramic grain boundaries. In this context, a statistically meaningful characterization of the viscous properties of grain boundaries can be obtained. In addition, we shall show that this internal friction technique can also be used to classify individual types of grain boundaries and to classify their different viscosity characteristics, provided that an adequate analysis of the grain-boundary peak morphology has been performed as a function of the grain size of the polycrystal. The above items of information confer on the internal friction technique a unique experimental resolution in studying grain-boundary viscosity and its related phenomena. In a more general view, we consider internal friction as an experimental technique with the potential characteristics of mechanical spectroscopy.

II. EXPERIMENTAL

A. Polycrystalline ceramic oxides

Al_2O_3 and MgO polycrystalline bodies were prepared in a disk shape with diameter and thickness of ≈60 and 6 mm, respectively, using a pressureless sintering techniques. The starting Al_2O_3 powder (AKP-HP, Sumitomo Chem., Co., Tokyo, Japan) has an average size in the range 0.3–0.6 μm and a degree of purity >99.995% (Si<8 ppm, Na<3 ppm, Mg<3 ppm, Fe<8 ppm, Cu<3 ppm). The average particle size of the starting MgO powder (100A, Ube Industries, Ltd., Ube, Japan) was in the range 0.010–0.014 μm and the degree of purity >99.98% (Al<10 ppm, Si<20 ppm, Ca<20 ppm, Fe<10 ppm, Zn<70 ppm, Na<10 ppm, Mn<10 ppm). Sintering was performed in air at 1873 K for 1 h. No secondary phases or densification additives were added. According to the above sintering schedule, all the ceramic specimens were sintered up to nearly theoretical density (>98%). Rectangular bars for internal friction tests were then obtained (in dimensions $2\times3\times50$ mm) from the sintered disks by successive procedures of diamond cutting, grinding and polishing. The average grain size was determined by optical microscopy on polished and thermally etched surfaces, according to the random interception method proposed by Hilliard and Cahn.[20] The average grain size of the as-sintered Al_2O_3 and MgO polycrystalline specimens were 3.3 and 5.0 μm, respectively. In order to investigate the effect of grain growth on both the morphology and the shift of the internal friction peak, annealing cycles were performed for 5 to 120 h at 1873 K. The largest average grain size obtained for both ceramics investigated was ≈25 μm. Larger grain sizes could, in principle, be obtained by selecting higher annealing temperatures or longer holding times. However, in the present ceramics, a grain size larger than ≈25 μm (particularly in Al_2O_3) developed spontaneous grain-boundary microcracking upon cooling from the annealing temperature. To minimize the statistical scatter in comparing the grain-boundary structures of polycrystals with different grain sizes, the same individual internal friction bar was tested after performing repeated annealing cycles. Given the relatively short term exposure to the high temperature necessary for completing an internal friction run, no detectable difference in grain size could be found when comparing the polycrystals before and after testing.

B. Internal friction experiments

In this study, internal friction was measured by the free-decay method,[21] using a torsion pendulum device equipped for high-temperature measurements. This pendulum utilized the structure designed by Kê[22] and enabled measurements at frequencies in the range $f=1-30$ Hz. The pendulum device was of an inverted type, with the ceramic specimen rigidly clamped at its lower end and attached at the upper end to a metallic bar with a relatively large inertia. Mechanical oscillations of the specimen were detected through the frequency modulation of an electric signal applied to the plates of a condenser. According to the experimental procedure proposed by Salvi *et al.*,[23] continuous recording was obtained by attaching one condenser plate to the oscillating inertia bar, while the other plate was attached to a fixed support. Concurrently, strains were detected by a high-sensitivity eddy-current-type displacement meter with a precision better than $\pm4.0\times10^{-4}$%. The entire torsion pendulum device was enclosed in a vacuum-tight ambient in order to perform experiments in a controlled atmosphere. All the present internal friction tests were conducted in an inert Ar atmosphere. Temperature was gradually increased during the internal friction experiments using a carbon heater rolled around the ceramic specimens. Both a thermocouple and an infrared thermoanalyzer were used for temperature measurements, depending on the measurement range. Cooling of the metallic grips which clamp the specimen was obtained by external cooling jackets. The free-decay oscillation was automatically measured at intervals of ≈5 K and the logarithmic decrement of free vibration was calculated. Internal friction Q^{-1} is a dimensionless parameter which measures the rate of free decay after an initially applied pulse stress, according to the following equation:

$$Q^{-1}=(1/\pi)\ln(A_n/A_{n+1}). \tag{1}$$

Here the argument of the natural logarithm represents the ratio between the amplitudes of two successive free oscillations of the specimen, e.g., the logarithmic decrement of free vibration; the higher the ratio, the higher the internal energy dissipation. The shear modulus was also calculated from the free-decay decrement, according to the method described by Nowick and Berry.[21] A more detailed description of both the torsion pendulum and the internal friction measurements has been given in a previous report.[24]

III. THEORY

A. Grain-boundary structure and width in ceramic oxides

Despite the recent advances in experimental microscopy techniques[25] and theoretical simulations[26] in probing and modeling the grain-boundary structure of ceramics with increasing resolution, the ultimate structure of grain bound-

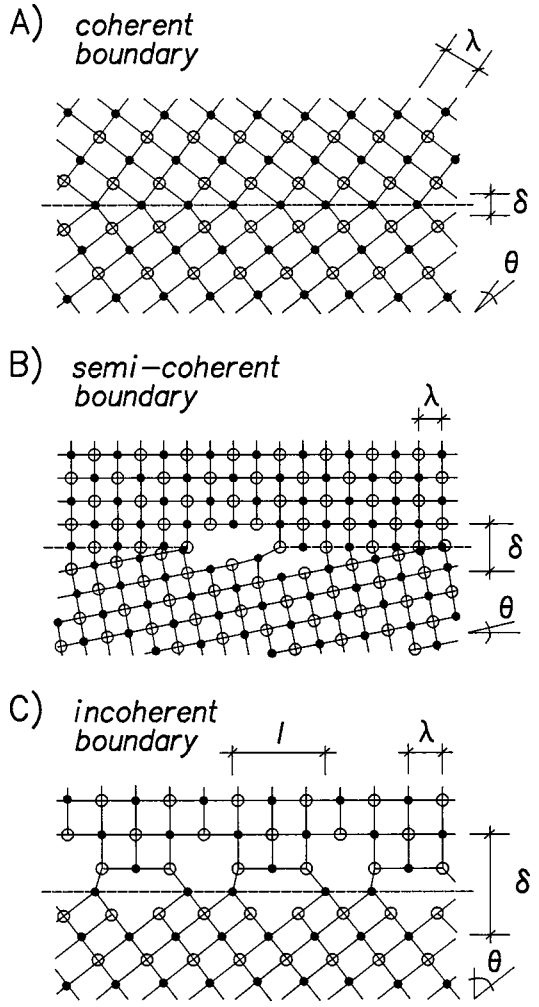

FIG. 1. Schematic of coherent, semicoherent, and incoherent grain boundaries in the simple case of a cubic oxide structure. The salient geometrical parameters are indicated.

aries at the atomic level in ceramics is still poorly understood, especially for complex crystal structures.

The general description of a directly bonded grain boundary in three dimensions requires the specification of the orientation of both the adjacent crystals, involving thus the knowledge of three independent angles. In addition, the orientation of the boundary plane relative to one of the crystals, which implies the choice of two additional angles as further independent variables, is necessary. Thus, the general three-dimensional grain boundary is characterized by five degrees of freedom. In a simplified view, a random bidimensional section of the grain boundary identifies a misfit angle θ between the main crystallographic direction of two neighboring grains. According to the misfit angle θ grain boundaries are usually classified into three categories.[27] If θ is small (i.e., 0°–15°), the boundary is called the *coherent* boundary [Fig. 1(A)], and geometrically coincides with a dislocation array.[28] With increasing the misfit angle θ the grain boundary will approach a fully incoherent structure, in which a one-to-one matching of the lattice planes across the boundary is lost. In this view, two additional classes are considered to be the *semicoherent* [Fig. 1(B)] and the *incoherent* boundaries [Fig. 1(C)]. Semicoherent boundaries present lattice strains since the lattice planes must be ''bent'' to give the one-to-one matching, while in incoherent boundaries the regularity of lattice-plane matching across the boundary is lost. If the width δ of a directly bonded grain boundary is defined as the thickness of the surface layer where a disturbed structure is present, it follows that the higher θ, the larger δ.

The statistical occurrence of fully coherent grain boundaries should be considered to be necessarily limited to a small fraction of the entire grain-boundary population in the polycrystal, the more complex the crystal structure the lower the fraction.[29] It can be theoretically demonstrated that less than 10% of all the grain boundaries are small-angle boundaries, because the probability that all three orientation angles are low is very small.[28] A statistical analysis of grain-boundary orientation in high-purity polycrystalline Al_2O_3 has been recently reported by Cho *et al.*[30] based on electron backscattered Kikuchi diffraction technique. In this study, a large number of grains could be analyzed, thus leading to statistically meaningful results. It was shown that grain boundaries with a misorientation $<15°$ were only $\approx 3\%$ of the total grain-boundary population. In addition, these authors showed an analysis of coincidence-site-lattice (CSL) grain boundaries, classified according to the Brandon's multiplicity criterion.[31] The proportion of such special boundaries in Al_2O_3 was rather low, the CSL boundaries being mainly observed between smaller grains. This latter observation would imply that the CSL boundaries in Al_2O_3 are those with the lowest mobility within the entire grain-boundary population of the polycrystal. The fraction of fully coherent boundaries in Al_2O_3 can be significantly enhanced (i.e., up to $\approx 30\%$ CSL boundaries) by adding Mg dopant.[32] However, this should not be the case of the present high-purity Al_2O_3 whose content of Mg impurity was <3 ppm. Another important output of the electron backscattered analysis was that the fully incoherent grain boundaries in alumina ($\theta > 85°$) constituted a fraction of $\approx 10\%$ of the entire population in the polycrystal.

Similar to their geometrical arrangement, the rate of self-diffusion in individual grain boundaries of ceramic oxides is expected to be strongly influenced by the misfit angle θ. Coherent boundaries have the closest structure to the bulk lattice, and minimum δ. Thus, their diffusion coefficient is expected to be the closest to the coefficient of bulk diffusion. Given the inverse proportionality relationship between diffusivity and viscosity, low-angle boundaries should experience the highest viscosity within the boundary population of the polycrystal. On the other hand, a parallel array of open pipes in the core structure of highly incoherent boundaries (i.e., with large θ) (cf. Fig. 1) that may act as rapid diffusion paths,[15] these boundaries thus having a low intrinsic viscosity. Duffy and Tasker[33] have quantitatively discussed the structure of high misfit angle boundaries in MgO and shown, by an atomistic simulation technique, that the width of the dislocation pipes at grain boundaries of MgO may reach the size of several lattice widths.

It is expected that the higher the diffusion characteristics of the grain boundaries, the higher their mobility upon grain growth. Thus, incoherent boundaries should selectively disappear first upon high-temperature annealing. Carter and Morissey[34] have used the generalized coincident-site-lattice theory proposed by Wagner *et al.*[35] to discuss the grain-boundary structure of Al_2O_3. Their studies have proved that

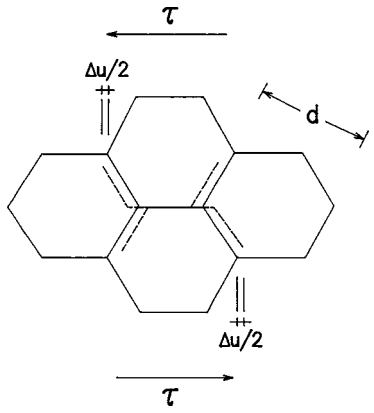

FIG. 2. Schematic and salient parameters of the mechanism of recoverable sliding at grain boundaries of directly bonded ceramic.

an Al_2O_3 grain facet with open structure will migrate much faster than a densely packed one. According to the above statements, annealing cycles and grain coarsening should reduce the average grain-boundary thickness and/or increase their inherent viscosity, as compared to a fine-grained polycrystal.

B. Grain-boundary viscosity of ceramic oxides

Internal grain boundaries in polycrystalline solids are a source of internal energy dissipation which may arise from their viscous slip at elevated temperatures[18] (Fig. 2). With increasing temperature, the grain boundaries become viscous and cannot sustain a shear stress. Local slip occurs until the stress at grain boundaries has been locally released. When the applied stress is sufficiently low, no microcracking or cavitation damages occur at grain boundary. Therefore, upon releasing the applied stress, the elastic deformation of the neighboring ceramic grains will be recovered and grain boundaries will be pushed back to their original position. The polycrystalline structure will be then restored to its original undeformed state. The elastic deformation of the bulk ceramic grains dictates the magnitude of the (constrained) grain-boundary slip which, according to the inherent viscosity of the grain boundary, must occur within a finite time, t^*.

Let us consider a macroscopic shear stress (i.e., a torque) which is applied to the polycrystal as a sinusoidal pulse wave of maximum stress τ and frequency, f. Upon monitoring the free decay of the polycrystalline specimen oscillation, the occurrence of recoverable grain boundary sliding leads to the presence of a peak in the $Q^{-1}(T)$ curve. The initial stress pulse activates the microscopic (elastic) displacement of the ceramic grains and viscous grain-boundary sliding eventually takes place according to the particular applied frequency (cf. Fig. 2). In absence of external frictions, the amplitude of the free oscillation must reduce due to viscous energy dissipation. Two parameters enhance the rate of internal energy dissipation, Q^{-1}: (1) the length Δu over which the reciprocal sliding between grains occurs, and (2) the intrinsic viscosity η_{gb} of the grain boundary. Due to the competing roles of these two parameters, a relaxation peak, located at $T=T_p$, is found in the $Q^{-1}(T)$ curve as temperature increases. A detailed description about the origin of the internal friction peak in polycrystalline ceramics has been given in a previous paper.[36]

The maximum (elastic) displacement allowed by the neighboring grains is proportional to the average grain size d and to the elastic shear strain, $\gamma=\tau(1-\nu)/G$, where ν and G are the Poisson's ratio and the shear modulus of the bulk ceramic crystallites, respectively. Assuming that G equals the macroscopic shear modulus of the unrelaxed polycrystal, G_U, it follows that

$$\Delta u_{\max}=\alpha d\tau(1-\nu)/G_U, \tag{2}$$

where α is a proportionality constant related to the microstructural morphology of both grains and grain boundaries.[37] The viscosity of the grain boundary channel η_{gb} at the internal friction peak temperature T_p is given by[38]

$$\eta_{gb}=\tau\delta(t^*/\Delta u_{\max})=G_U\delta/2\pi f\alpha(1-\nu)d, \tag{3}$$

where δ is the grain-boundary thickness. Note that, according to Eq. (3), a change in grain size d of the specimen will have the same effect as a change of the vibration frequency, f. This is because the relaxation time associated with the stress relaxation across grain boundaries increases proportional to an increase in grain size. In presence of a larger grain size, a larger relative displacement can occur at grain boundaries before it is blocked at the grain edges and corners (cf. Fig. 2). Thus, a longer time will be required to reach $\Delta u_{\max}$. On the other hand, when the frequency of vibration is kept constant, an increase in grain size will shift the internal friction peak to higher temperatures.

The morphology parameter α can be expressed in terms of experimentally accessible parameters, according to the following considerations. The total macroscopic shear strain γ of the polycrystal loaded by τ at the temperature T_p consists of the sum of an elastic component and an anelastic component arising from the elastic deformation of the bulk grains and the viscous sliding at grain boundaries, respectively,

$$\gamma=(\tau/G_U)+(\Delta u_{\max}/d)=\tau/G_R, \tag{4}$$

where G_R is the macroscopic shear modulus of the polycrystal after relaxation by grain-boundary sliding at the temperature T_p. Substituting from Eq. (2) and rearranging, the morphology factor α can be expressed as

$$\alpha=[(G_U/G_R)-1]/(1-\nu), \tag{5}$$

where the relaxation modulus ratio G_U/G_R at the peak-top temperature is now an experimentally accessible parameter. In addition, it can be shown that, at $T=T_p$, the modulus ratio G/G_R is related to the height of the internal friction peak $Q^{-1}_{\max}$, through the following equation:[21]

$$G_U/G_R=1/[1-(Q^{-1}_{\max}/2)]. \tag{6}$$

High-purity oxide ceramics usually show directly bonded grain boundaries whose thickness is unfortunately neither constant nor clearly visible by electron microscopy. It was discussed in the previous section that δ in ceramic oxides may significantly vary according to the neighboring grain

orientation. Normalizing by the thickness δ and substituting for α from Eqs. (6) and (7), one obtains

$$\eta_{gb}/\delta=(G_U/2\pi fd)[1-(Q_{max}^{-1}/2)]/(Q_{max}^{-1}/2). \quad (7)$$

Equation (7) is valid only at $T=T_p$ and represents the basic relationship which links the measured internal friction peak characteristics with both the intrinsic grain-boundary viscosity and the microstructural parameters of the ceramic polycrystal.

An important implication in using Eq. (7) is that a variation of either grain size or oscillation frequency should produce a well-defined temperature shift of the internal friction peak. This phenomenon can be used to obtain an Arrhenius plot of the η_{gb}/δ parameter and to calculate from its slope an activation energy (peak-shift method). With this activation energy information at hand, we may attempt to discuss the elementary process behind grain-boundary sliding in oxide ceramics. As an alternative, the activation energy for the thermally activated grain-boundary sliding can be obtained from the width W of the internal friction peak (peak-width method), according to the following equation:

$$H=2(\cosh^{-1}2)R/W, \quad (8)$$

where R is the gas constant and H an activation energy for the phenomenon through which the peak is originated. However, Eq. (8) should be considered to be valid only under the hypothesis that the experimentally determined internal friction peak arises from a single-relaxation phenomenon or, in other words, if the peak is a Debye peak. The experimental peaks usually arise from a relaxation spectrum and the implications of this characteristic are discussed in detail in the following sections. Measurements of internal friction as a function of temperature, frequency, and grain size will now be considered as a means of deriving experimentally the intrinsic grain-boundary viscosities of high-purity Al_2O_3 and MgO ceramics.

IV. RESULTS

The internal friction curve as a function of temperature T was recorded at different oscillation frequencies and grain sizes. The experimental $Q^{-1}(T)$ curves of all the polycrystalline specimens investigated in this study could be deconvoluted into two components: (1) an exponential-like background component; and, (2) a peak component. The $Q^{-1}(T)$ curves and the deconvolution procedure is shown in detail in the Appendix. The background component was subtracted from the experimental $Q^{-1}(T)$ curve to single out the anelastic peak component.

The anelastic peak component of internal friction was analyzed in this study because it has been shown to be directly related to the viscous behavior of grain boundaries.[18,19] In addition, in a previous study on sapphire and MgO single crystals,[24] it was shown that no significant relaxation due to dislocation motion occurred in either crystal at the (low) stress level in the temperature range investigated in this paper.

Figures 3(A) and 3(B) show the evolution of the grain-boundary peak component of internal friction in Al_2O_3 and MgO, respectively, as a function of the average grain size of

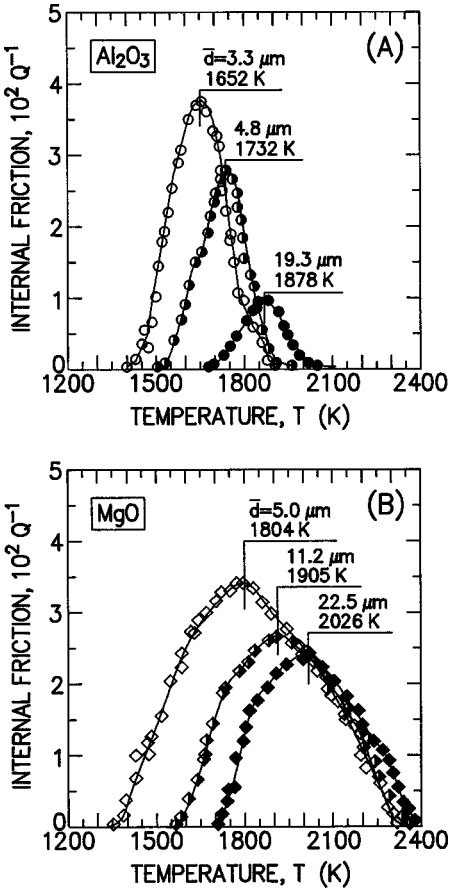

FIG. 3. Grain-boundary peak component of internal friction as a function of grain size in Al_2O_3 (A) and MgO (B) polycrystals.

the polycrystal. In both the oxides, the increase in grain size (upon annealing) has a threefold effect on the grain-boundary relaxation peak: (1) it reduces the peak intensity, (2) it shifts the peak toward higher temperatures, and (3) it alters the peak morphology, in particular by reducing the peak width.

The reduction of peak intensity upon grain growth is clearly related to a reduction of the grain-boundary area per unit volume. This implies a lower internal energy consumption within one oscillation period because the amount of boundary surface actually undergoing sliding is reduced. The absolute intensity of the grain-boundary peaks in the polycrystals with the smallest grain size is very similar both in Al_2O_3 and MgO. However, the reduction of peak intensity associated with grain growth is much more pronounced in Al_2O_3.

At larger grain sizes, a shift toward higher temperatures is actually predicted by Eq. (7), according to which a larger d value would imply a lower viscosity value η_{gb} experienced at the temperature of peak maximum. As discussed in the previous section, a larger grain size will imply a larger relative displacement at grain boundaries before sliding is blocked at triple-grain junctions, therefore a longer time is required to cover this larger sliding distance. Equation (7) also predicts the same reduction of η_{gb} at an increase in oscillation frequency, f. This trend was indeed found experimentally in both the ceramic oxides investigated, as shown in Figs. 4(A) and 4(B) for these fine-grained materials. Systematic shifts toward higher temperatures arising from an

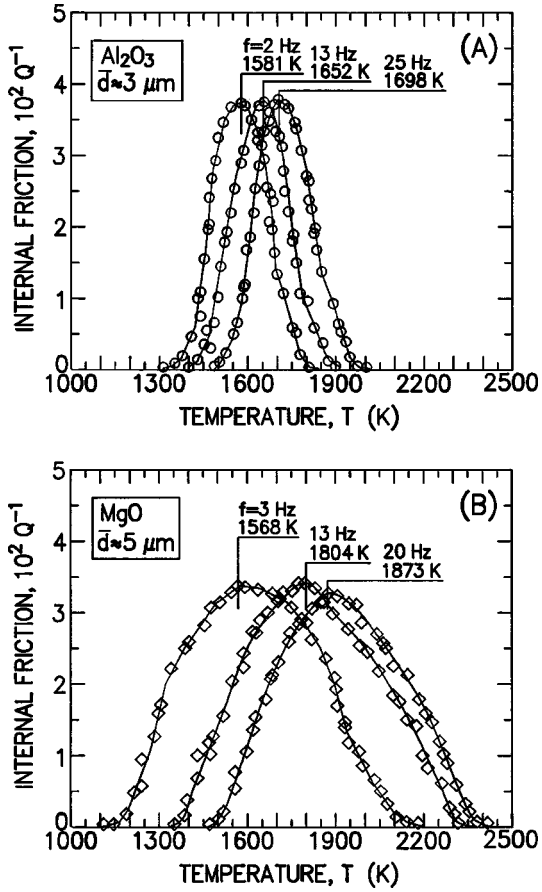

FIG. 4. Shift of the grain-boundary peak component of internal friction upon changing the frequency of torsional oscillation in fine-grained Al_2O_3 (A) and MgO (B).

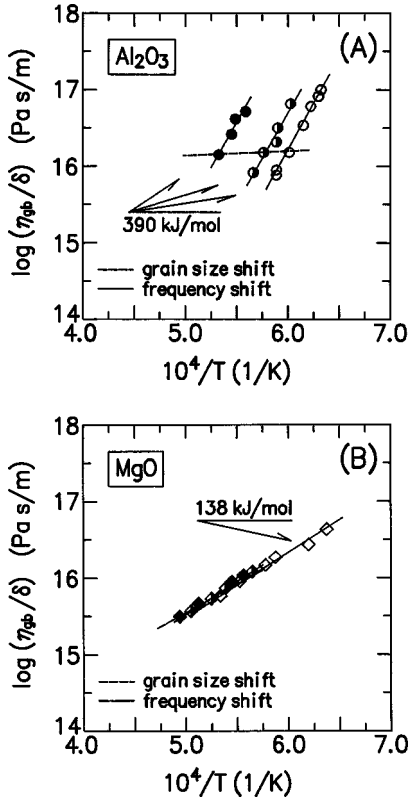

FIG. 6. Arrhenius plots of grain-boundary viscosity per unit thickness, as determined according to Eq. (7) as a function of frequency and grain size, are given for Al_2O_3 and MgO polycrystals in (A) and (B), respectively. Apparent activation energy values are also shown. The errors involved in these measurements are ± 30 and ± 20 kJ/mol for Al_2O_3 and MgO, respectively.

increase of frequency were found in both Al_2O_3 and MgO, independent of grain size. After calculating the grain-boundary morphology factor α according to Eqs. (5) and (6) (Fig. 5), the grain-boundary viscosity per unit grain-boundary thickness η_{gb}/δ, was calculated according to Eq. (7). The complete sets of results obtained at different grain sizes and frequencies are plotted in Arrhenius fashion for the Al_2O_3 and MgO polycrystals in Figs. 6(A) and 6(B), respectively. In comparing the behaviors of these two oxides, an important difference can be noticed. In MgO, variations of both d and f produce shifts of the η_{gb}/δ value consistent with a unique Arrhenius plot [Fig. 6(B)]. On the other hand, three distinct plots are found in Al_2O_3 by varying the frequency in polycrystals with different grain sizes [Fig. 6(A)]. This is an important characteristic which implies important differences in the viscous behavior of the grain boundaries in these two ceramic oxides. However, it is important to note that, although three distinct Arrhenius plots can be generated in Al_2O_3 upon frequency shift for different grain sizes, all the plots have the same slope, corresponding to an activation energy, $H \approx 390 \pm 30$ kJ/mol [cf. Fig. 6(A)]. This means that a common elementary mechanism is behind the thermally activated grain-boundary sliding, indipendent of grain size. The activation energy of the single plot of MgO [in Fig. 6(B)] is found to be $H \approx 140 \pm 20$ kJ/mol, a value significantly lower than that of Al_2O_3. The activation energy found for the Al_2O_3 polycrystal may agree with the grain-boundary diffusion of either Al (Ref. 39) or O.[40] However, Cannon *et al.*[41] estimated that Al is the slower diffusing species in polycrystalline Al_2O_3, thus controlling the deformation rate. In MgO polycrystal, analysis by the oxygen-isotope exchange-reaction method showed similar activation energy as that found in the present experiments.[42] Therefore, atomic diffusion along the pipe structure of directly bonded grain boundaries is henceforth assumed to be the predominant elementary mechanism involved in the grain-boundary mobility and sliding in both the studied oxides.

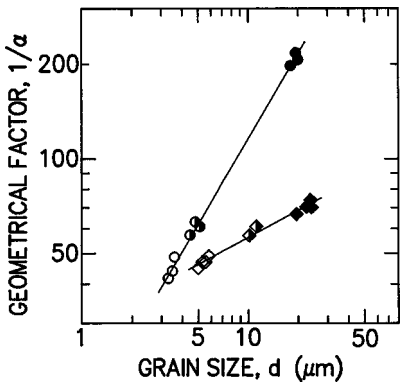

FIG. 5. Plot of the geometrical factor, α, as calculated according to Eqs. (5) and (6), as a function of the average grain size of the polycrystals. The symbols are the same as those in Fig. 3.

To quantify the variation of peak morphology, the peaks

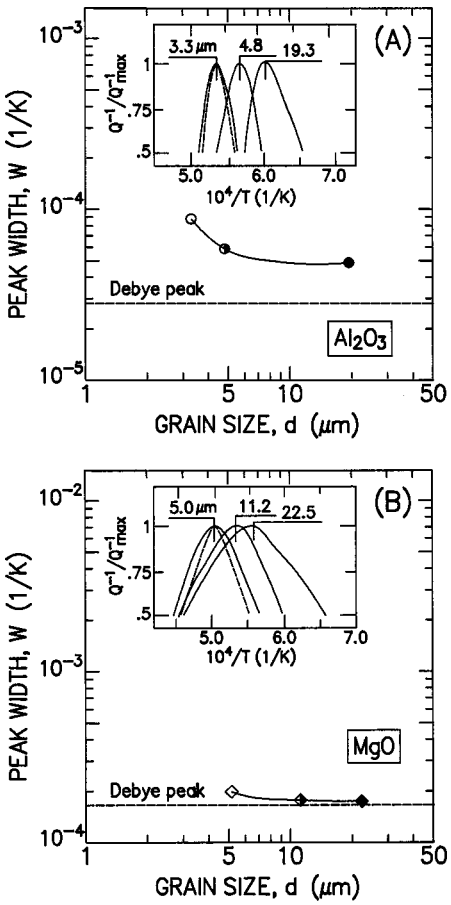

FIG. 7. Plots of experimental peak width of Al_2O_3 (A) and MgO (B), as a function of the average grain size of the polycrystals are compared with the width of the respective Debye peak calculated according to Eq. (8). The normalized grain-boundary peaks and the Debye peaks are shown in the respective insets.

are normalized with respect to their height and their full width at half maximum W plotted as a function of grain size. The results of this analysis are summarized in Figs. 7(A) and 7(B) for Al_2O_3 and MgO, respectively. The peak of MgO at any grain size is significantly broader than the peak of Al_2O_3 because the elementary phenomenon of grain-boundary diffusion in MgO has an activation energy lower than in Al_2O_3 [cf. Fig. 6 and Eq. (8)]. Upon grain growth, the grain-boundary relaxation peak of both the oxides approaches the width of a single-relaxation peak (or a Debye peak). In this context, it is noteworthy that the activation energies calculated by the peak width method [i.e., according to Eq. (8)] for the materials with the largest grain size agree with the respective activation energies obtained by the peak shift method from Figs. 6(A) and 6(B) within a 10% error. Provided that a sound explanation can be given for the the reduction of W upon grain growth, the agreement between the activation energies obtained by peak-shift and peak-width methods may prove the self-consistency of the present internal friction approach. This result is regarded as an encouraging starting point for the peak-morphology analysis presented in the next section.

V. DISCUSSION

A. Analysis of peak morphology and grain-boundary thicknesses

As discussed in Sec. III, a ceramic polycrystal contains a regular collection of grain boundaries along which energy dissipation by viscous slip may occur. It can be assumed that the spheres of relaxation of individual grain boundaries do not significantly overlap, which implies each grain boundary will respond to external stress independent of its neighbors. However, the grain-boundary peak of internal friction is given by the superposition of contributions from individual sets of internal boundaries having the same characteristics. This is because each grain boundary within the same directly bonded polycrystal has a certain thickness (i.e., misfit angle), a certain intrinsic viscosity dictated by its particular structure, and is formed between grains of various sizes. Any variation of these characteristics may, in principle, affect the temperature range and/or the morphology of the peak. When experiments are performed at a fixed oscillation frequency, Eq. (7) suggests that an internal distribution of either grain sizes d or grain-boundary thicknesses δ may give rise to a set of individual peak components, whose intensity is proportional to the statistical occurrence of that particular boundary population.

A quantitative analysis of the effect of grain size distribution on the grain-boundary peak morphology has been performed by Feltham.[43] This basic study shows that the contribution to peak widening, which may result from the diameter distribution of the grains, is much lower than that which is actually found in our experiments. This may disprove the thesis of a significant peak-width dependence on grain size distribution in the present ceramic oxides. In addition, similar evolutions of the grain-size distribution in Al_2O_3 and MgO upon annealing, should give rise to similar morphological changes of the internal friction peak, which is not the present case, as shown in the remainder of this section.

On the other hand, we have stated in Sec. III A that the grain-boundary width δ in directly bonded ceramic oxides may vary by more than one order of magnitude upon varying the misfit angle, θ. In addition, a pronounced increase of diffusivity is expected at high θ angles. Therefore, a variety of possible diffusion-pipe structures in directly bonded ceramic grain boundaries may originate a relaxation spectrum which broadens the internal friction peak, as compared with a single-relaxation Debye peak. With this in mind, a deconvolution analysis in individual components is attempted for all the grain-boundary peaks shown in Figs. 3(A) and 3(B).

Figures 8(A)–8(C) and 9(A)–9(C) represent the grain-boundary peaks at various grain sizes of Al_2O_3 and MgO, respectively, normalized relative to their respective peak heights and deconvoluted into individual peak components. A common structure of the grain-boundary relaxation peak is recognized in both the oxides: the grain-boundary peak of polycrystals with the finest grain size can be deconvoluted into three main components. Two major components of similar height and width are located at lower temperatures, and a minor component is centered at a higher temperature. The components belonging to the doublet have a larger width but

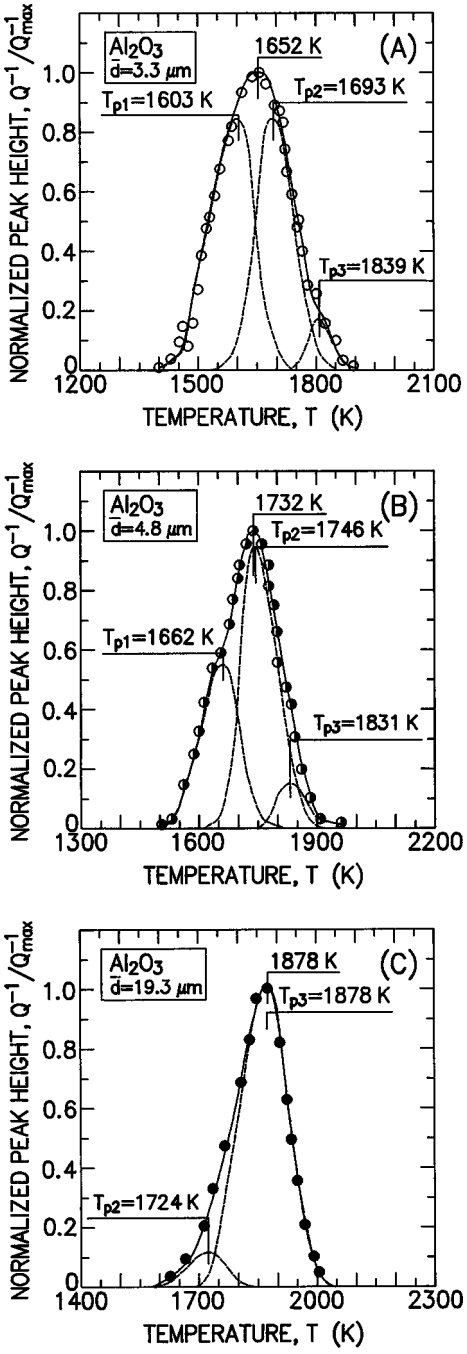

FIG. 8. Deconvolution analysis of the normalized grain-boundary peak of internal friction for the Al_2O_3 polycrystal, as a function of grain size.

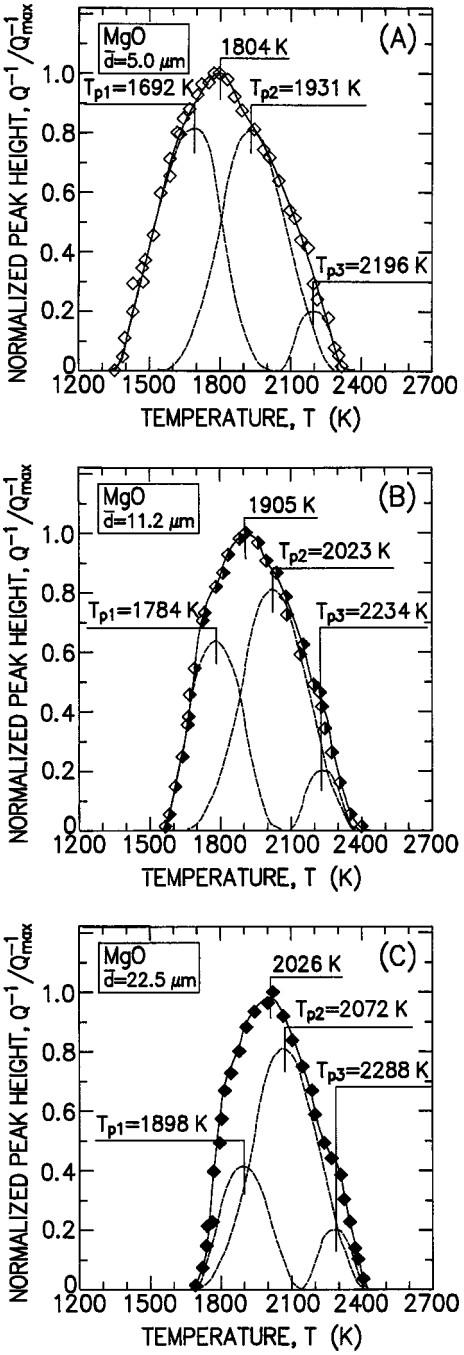

FIG. 9. Deconvolution analysis of the normalized grain-boundary peak of internal friction for the MgO polycrystal, as a function of grain size.

are reasonably close to the respective Debye peaks [i.e., those drawn by accounting for the activation energy determined by the peak-shift method in Figs. 7(A) and 7(B)]. The minor component has in both the oxides an activation energy very close to that of a Debye peak. Upon grain growth, the component of the peak doublet which is centered at the lower temperature (denominated T_{p1} component, henceforth, where T_{1p} represents the temperature at peak maximum) tends to disappear in both materials, and it totally disappears in the Al_2O_3 with $d \geqslant 20\,\mu$m. Also in Al_2O_3 the intensity of the high-temperature component of the doublet (T_{p2} component) significantly decreases with increasing grain size. On the other hand, the minor peak (T_{p3} component) is very stable and maintains a constant intensity upon annealing. In MgO, both the T_{p2} and T_{p3} components are rather stable upon grain growth.

In this paper, we propose that the T_{p1}, T_{p2}, and T_{p3} peak components arise from sliding of three kinds of grain boundaries: (1) the fully incoherent, (2) the semicoherent and, (3) the coherent grain boundaries, respectively. This interpretation may seem at first sight to be a rather simplistic one, considering that a very large variety of grain boundaries should be available in a polycrystal. However, this idea is supported by the following qualitative considerations: (1) the fraction of fully coherent boundaries is quite low,[30] due to

the very small probability of three orientation angles between neighboring crystals being low. This characteristic is represented by the limited height of the T_{p3} component in both oxides; (2) the higher the degree of coherency of a set of boundaries the higher the temperature range at which their peak component manifests, consistent with a higher intrinsic viscosity and/or a lower thickness [cf. Eq. (7)]; (3) the fully incoherent boundaries (represented by the respective T_{p1} components) represent a minor fraction of the grain-boundary population (according to the experimental analysis in Ref. 30) and tend to disappear first upon grain growth, while coherent boundaries (T_{p3} components) are very stable; and, (4) in the more complex grain-boundary structure/variety of the hexagonal A_2O_3 (vs cubic MgO), a larger fraction of incoherent grain boundaries disappears upon grain growth. In addition, the semicoherent boundaries of cubic MgO are relatively more stable upon annealing.

Let us start from the above latter observation and assume in a first approximation that the coefficient of oxygen self-diffusion at grain boundaries is independent of the misfit angle θ. This assumption would imply that the rate of grain-boundary sliding is mainly dictated by the geometry of pipe structure and, in particular, the thickness of the grain boundary. A similar assumption has been proposed for metallic grain boundaries.[15] This should be particularly true in comparing coherent and semicoherent boundaries (i.e., at relatively low θ). In fact, although the semicoherent boundaries should present lattice strains to give the one-to-one atomic matching, they are thought to preserve a regular structure resembling that of coherent boundaries, without large dislocation pipes [cf. Fig. 2(B)]. This hypothesis is also supported by their relatively low mobility upon annealing (cf. T_{p2} components in Figs. 8 and 9). For a low θ angle in coherent boundaries, $l \approx \lambda \approx \delta$. If the two classes of coherent and semicoherent boundaries have a comparable intrinsic viscosity, then the shift toward lower temperature of the peak component T_{p2} with respect to T_{p3} should be entirely due to an increase in grain-boundary thickness, δ. According to a linear dependence $\ln(\eta_{gb}/\delta)$ vs $1/T$ and assuming a unique η_{gb} value among different kinds of boundaries, it follows that $\ln(\eta_{gb}/\delta_2) - \ln(\eta_{gb}/\delta_3) = \ln(\delta_3/\delta_2) = H[(1/T_{p2}) - (1/T_{p3})]$. Thus, using the respective values of activation energy H from the plots in Figs. 6(A) and 6(B) and taking the interval $[(1/T_{p2}) - (1/T_{p3})]$ from Figs. 8 and 9 for Al_2O_3 and MgO, respectively, the grain-boundary thickness of the the semicoherent boundaries can be calculated. By doing so, a widening of δ is found in both oxides for semicoherent boundaries, as compared with the respective coherent structures. For coherent grain-boundary structures with $\delta_3 \approx \lambda = 5.60$ Å and 4.21 Å (in Al_2O_3 and MgO, respectively) the correspondent average thicknesses of the semicoherent grain boundaries δ_2 are $\approx$100 Å and $\approx$12 Å, respectively. Note that the much larger widening of Al_2O_3 boundaries with respect to that of MgO is consistent with both the more complex crystal structure of Al_2O_3 (i.e., hexagonal vs cubic MgO structure) and the more rapid disappearance of the T_{p2} peak component (i.e., the higher grain-boundary mobility) found in Al_2O_3 upon annealing.

It may be possible to extrapolate to large θ angles the hypothesis of a constant intrinsic viscosity of grain boundaries, but at present we are unable to test it. This hypothesis

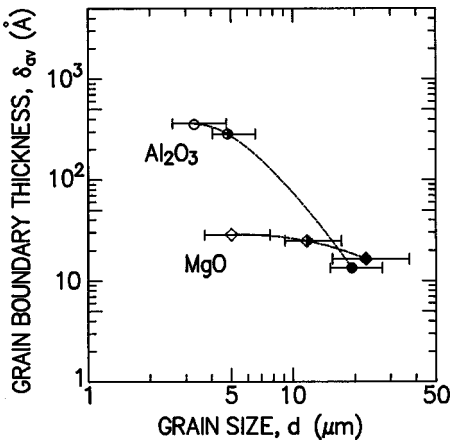

FIG. 10. Average grain-boundary thickness as a function of grain size in Al_2O_3 and MgO polycrystals. As explained in Sec. V, these plots represent un upper limit for the grain-boundary thickness of both oxides.

may also lead one to consider that the shift of the T_{p1} component at lower temperature is entirely due to grain-boundary widening. Nevertheless, a more mechanistic view of the grain-boundary layer would suggest that the presence of an array of ''holes'' (i.e., large diffusion pipes) at grain boundaries should lead to a lower average viscosity for the matter within this layer. This can be still consistent with the hypothesis of a constant diffusivity into the individual pipes, independent of their size. We leave aside this somewhat semantic problem, but note that the present estimate of grain-boundary thickness only represents an upper limit value; the larger the θ angle, the higher the overestimation of δ. A calculation of the grain-boundary thickness, δ_1, for the T_{p1} component (performed in a similar way as done above for the T_{p2} component), leads to the values $\delta_1 \approx 680$ and 50 Å in Al_2O_3 and MgO, respectively. Figure 10 shows the average grain-boundary thickness δ_{av}, as a function of the average grain size d for both Al_2O_3 and MgO polycrystals. δ_{av} was calculated as an arithmetic mean of δ_1, δ_2, and δ_3, weighted by the relative intensities of the respective peak components shown in Figs. 8 and 9. In the Al_2O_3 with $d = 4.8\,\mu$m, $\delta_{av} \approx 280$ Å, which is reasonably close to the value $\delta_{av} \approx 140$ Å calculated by Mistler and Coble[44] by comparing between sintering, grain growth, and creep data, although these authors do not specify the average grain size of their polycrystals. A closer observation of the $\delta_{av}(d)$ plot of Fig. 10 reveals a steep decrease (of about one order of magnitude) in the relatively narrow grain-size interval $4.8\,\mu\text{m} \leqslant d \leqslant 19.3\,\mu$m. The uncertainty in grain size may easily explain the difference by a factor of 2 between the Mistler and Coble's data and ours. Another explanation may be the possible overestimation of our δ data mentioned before, arising from the assumption of a constant viscosity among different classes of grain boundaries. A much weaker dependence of δ_{av} on grain size is found in MgO, which is consistent with its simple crystal structure. However, a value again larger by approximately a factor of 2 is found in comparing our data on MgO ($\delta_{av} \approx 23$ Å) with those determined by Ikuma and Komatsu[45] utilizing the oxygen-isotope exchange method ($\delta_{av} \approx 10$ Å at $\approx$1900 K). Eastman *et al.*[46] have proposed a electron-diffraction technique to directly determine the size

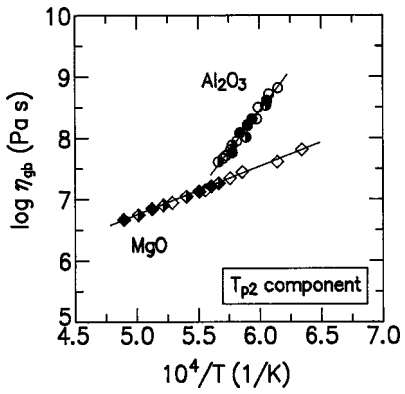

FIG. 11. Arrhenius plot of grain-boundary viscosity of semicoherent boundaries of both Al_2O_3 and MgO polycrystals. η_{gb} values have been calculated according to Eq. (7).

of grain-boundary dislocation pipes in NiO. Their high-resolution micrographs show a size of $l \approx 15$ Å for the dislocation-pipe structure of a $\theta = 12.25°$ tilt boundary. Given the fact that NiO and MgO have the same (rocksalt) type of cubic crystal structure, we may extrapolate the measurements on NbO to MgO to find agreement with the grain-boundary thickness determined in this study within an order of magnitude.

B. Intrinsic viscosities of grain boundaries

Semicoherent boundaries, represented by the T_{p2} component of the internal friction peak, should experience a unique Arrhenius plot with regard to their intrinsic viscosity, independent of the overall peak morphology. Invoking Eq. (7) to account for the effect of grain size, and using the values $\delta_2 \approx 100$ Å and 12 Å (as determined in the previous section) for Al_2O_3 and MgO, respectively, the (average) intrinsic η_{gb} of semicoherent boundaries can be calculated, independent of the particular polycrystal in which they are embedded. The Arrhenius plot of η_{gb}, relative to the T_{p2} peak component only, are displayed in Fig. 11, as obtained from data in Figs. 6(A) and 6(B). As seen, a unique Arrhenius plot of viscosity is obtained for both the oxides. Using the δ_{av} values in Fig. 10, also the viscosity values calculated from the T_{p1} and T_{p3} components can be shown to belong, within the experimental error, to the same linear plot of Fig. 11. This agreement should be regarded as a proof of internal consistency for the proposed internal friction method, because it shows that information about grain boundaries, which is obtained through the analysis of peak morphology, is the same as that obtained from a peak-shift analysis. However, this agreement does not add physical insight to the viscosity characteristics of different classes of grain boundaries, because the δ_{av} values shown in Fig. 10 were calculated under the hypothesis of constant η_{gb}. This means that, if the assumption of a constant intrinsic viscosity among different classes of boundaries breaks down, then the plots of Fig. 11 should be regarded as validly representing the viscosity trend only for the semicoherent class of boundaries. Looking at the schematics of various grain-boundary geometries in Fig. 1, it is also conceivable that incoherent boundaries possess a larger area of diffusion pipes, without necessarily having a significantly larger grain-boundary thickness. For example, Carter and Morrissey[37] have shown that coincident lattice sites in a typical high-angle boundary ($\theta = 27.8°$ about the [0001] axis) of Al_2O_3 are separated by a distance of $\approx 7\lambda$ across the boundary. Assuming this distance as the average grain-boundary thickness for the incoherent boundaries of Al_2O_3, an intrinsic viscosity value of ≈ 20 times lower is estimated for these boundaries, as compared with that of semicoherent boundaries shown in Fig. 11.

According to the above peak-width and peak-shift analyses, we can finally explain why the η_{gb}/δ data collected in MgO polycrystals with different grain sizes experience a unique Arrhenius plot [Fig. 6(B)], while the Al_2O_3 data does not [Fig. 6(A)]. There are two potential reasons: (1) the dependence of δ (or η_{gb}) upon the crystallographic misfit angle θ is much less pronounced in the MgO cubic structure as compared with the hexagonal Al_2O_3 (cf. Fig. 10); and, (2) the activation energy for ion diffusion at grain boundaries of MgO is less than one third that at grain boundaries of Al_2O_3, which makes the scatter due to δ of the viscosity value detected by internal friction less pronounced.

Unfortunately, grain-boundary viscosity data for Al_2O_3 and MgO polycrystals are not readily available in the literature at present, and a direct comparison with our data from the internal friction method is not possible. On the other hand, grain-boundary diffusivity data is available from various techniques for both the investigated oxides.[46–51] A comparison of this data from the literature shows that the ion self-diffusivity along the grain boundaries of Al_2O_3 is one to two orders of magnitude lower than that at the boundaries of MgO at temperatures 1600–1800 K, which is consistent with the higher grain-boundary viscosities of Al_2O_3 over MgO determined in the present study.

VI. CONCLUSION

Free-decay internal friction experiments were conducted on high-purity polycrystalline Al_2O_3 and MgO as a function of three independent variables: (1) temperature, (2) oscillation frequency, and (3) grain size. The grain-boundary peak components of the internal friction curves were discussed with emphasis on both the temperature shift and the peak-morphology changes occurring upon varying frequency or grain size. A model for recoverable grain-boundary sliding was used to quantitatively evaluate the viscous response of grain boundaries to an applied shear stress. An Arrhenius plot of grain-boundary viscosities was obtained for both Al_2O_3 and MgO polycrystals, according to a peak-shift analysis performed in the frequency range 2–25 Hz. Activation energies 390 ± 30 and 138 ± 20 kJ/mol were found for Al_2O_3 and MgO, respectively, which is consistent with the ion self-diffusion at grain boundary as the main elementary mechanism leading to sliding.

A deconvolution analysis of the grain-boundary relaxation peaks was performed at various (average) grain sizes in the range 3–23 μm. According to this latter analysis three main peak components could be identified, which were related to the sliding of three distinct classes of grain boundaries embedded in the polycrystal: (1) coherent, (2) semicoherent, and (3) fully incoherent grain boundaries. It has been shown that the grain boundaries with a low misfit angle contribute

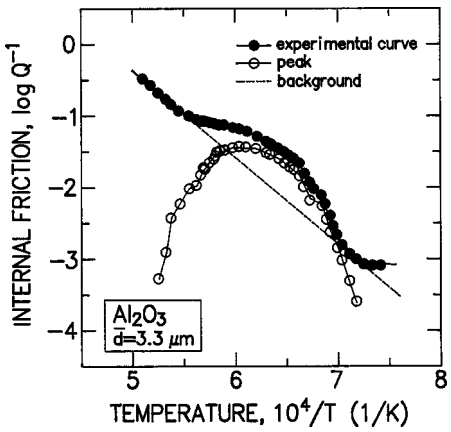

FIG. 12. Arrhenius plot of the experimental internal friction curve of fine-grained Al_2O_3 ($\approx$3.3 μm). The deconvolution procedure which enables to separate the background and the peak component is also shown.

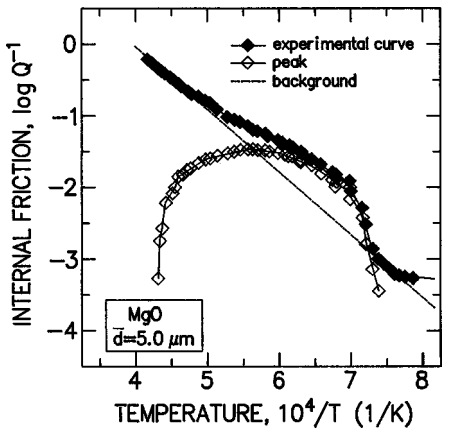

FIG. 13. Arrhenius plot of the experimental internal friction curve of fine-grained MgO ($\approx$5.0 μm). The deconvolution procedure which enables to separate the background and the peak component is also shown.

to the overall relaxation peak with a component T_{p3} located at higher temperature, which are very stable upon annealing. On the other hand, incoherent grain boundaries are represented by a low-temperature peak component T_{p1}, which tended to disappear upon annealing, meaning that incoherent boundaries disappeared with grain growth. Sliding of semicoherent boundaries gave rise to an intermediate internal friction component T_{p2} which, with grain growth, showed higher stability in MgO than in Al_2O_3. This behavior was consistent with the relatively simpler structure of grain boundaries in MgO cubic structure, as compared with hexagonal Al_2O_3.

The present internal friction analysis also allowed an estimate of an upper-limit value for the thickness of the various classes of grain boundaries, assumed to be the width of the path along which diffusion is significantly enhanced. An increase from the Å size of the thickness in coherent boundaries up to several nanometers in the semicoherent grain boundaries was found. This size estimation reasonably agreed with direct measurements of grain-boundary thickness performed by other authors by the oxygen isotope method or by various other indirect techniques. The magnitude of grain-boundary viscosity in the semicoherent class of boundaries was $\approx 10^8$ and 10^7 Pa$\times$s (at $\approx$1700 K), for Al_2O_3 and MgO, respectively. Incoherent grain boundaries in Al_2O_3 showed a maximum increase in thickness up to several hundred Å and/or a decrease in their inherent viscosity up to more than one order of magnitude as compared with higher coherency classes of boundaries.

ACKNOWLEDGMENTS

The author thanks Dr. K. Ota for his help with the experimental procedures. Professor T. Nishida, Professor T. Sakuma, and Professor Y. Ikuhara are sincerely acknowledged for many useful discussions.

APPENDIX

The experimental damping-temperature curves of polycrystalline metals are usually deconvoluted into two components, and exponential-like background and an anelastic peak.[21] However, this procedure is far from being established in polycrystalline ceramics. Here, we propose a procedure for deconvoluting internal friction spectra of ceramic oxides into the two above components and attempt to justify this procedure according to physically sound arguments.

In general, in ceramic as well as in metals, the background is much smaller in single crystals than in polycrystals, and is smaller in coarse-grained polycrystals (showing also smaller grain-boundary peaks) than in fine-grained samples. In analogy with metal polycrystals,[52] it can be thought that the background is of a viscoelastic nature. Besides recoverable grain-boundary sliding, the internal buildup of stress at the grain edges may also produce local (irrecoverable) plastic creep of a linear and thermally activated type, such that the specimen plastically deforms during internal friction test. This mechanism of plastic deformation may eventually be the same as that leading to creep under a constant stress. A complete analysis of the background component in comparison with the creep behavior of oxide ceramics is beyond the purpose of the present paper. However, to conceptually pool the phenomena behind creep and internal friction background would imply that the thermally activated background should obey an Arrhenius-like dependence on temperature, thus experiencing a straight line in an Arrhenius plot against the inverse of temperature.

Figures 12 and 13 show Arrhenius plots of the internal friction spectra collected on the finest grained Al_2O_3 and MgO polycrystals, respectively. The respective deconvolutions in peak and background components are also shown. It is clear from the above figures that it is actually possible to fit by a straight line the low- and high-temperature feet of the internal friction spectra of the present ceramic oxides. The spectra of the two oxides with the finest microstructure shown in Figs. 12 and 13, were the most difficult to deconvolute because they present very broad relaxation peaks. Nevertheless, straight lines can be clearly drawn and peak components singled out in an objective and reliable manner. Plotting and deconvoluting the internal friction spectrum in Arrhenius fashion involves two major advantages: (i) it makes it possible to precisely draw the background as the

straight line which best fits both high and low temperature internal friction data; and (ii) it highlights the actual morphology of the peak, which is discussed in the text. Thus, provided that data are collected in sufficiently short intervals of temperature ($\approx$5 K) and confirmed by several experimental runs, it is assumed that the morphology of the internal friction peak owns somewhat reliable morphological characteristics, as discussed in the text.

[1] B. J. Wuensch, in *Materials Science Research* (Plenum, New York, 1975), Vol. 9, p. 211.
[2] J. C. Fisher, J. Appl. Phys. **22**, 74 (1951).
[3] R. T. Whipple, Philos. Mag. A **45**, 1220 (1954).
[4] G. B. Gibbs, Phys. Status Solidi **16**, K27 (1966).
[5] K. Lehovec, J. Chem. Phys. **21**, 1123 (1953).
[6] R. B. Poeppel and J. M. Blakely, Surf. Sci. **15**, 507 (1969).
[7] S. K. Tiku and F. A. Kröger, J. Am. Chem. Soc. **63**, 183 (1980).
[8] W. D. Kingery, J. Am. Chem. Soc. **57**, 1 (1974).
[9] W. D. Kingery, J. Am. Ceram. Soc. **57**, 74 (1974).
[10] M. F. Yan, R. M. Cannon, H. K. Bowen, and R. L. Coble, J. Am. Ceram. Soc. **60**, 120 (1977).
[11] B. J. Wuensch and T. Vasilos, J. Am. Ceram. Soc. **49**, 433 (1966).
[12] A. Atkinson and R. I. Taylor, Philos. Mag. A **43**, 979 (1981).
[13] W. K. Chen and N. L. Peterson, J. Am. Ceram. Soc. **60**, 655 (1980).
[14] J. W. Osenbach and V. S. Stubican, J. Am. Ceram. Soc. **63**, 191 (1983).
[15] D. Turnbull and R. E. Hoffman, Acta Metall. **2**, 419 (1954).
[16] R. L. Coble, J. Appl. Phys. **34**, 1679 (1963).
[17] R. M. Cannon and R. L. Coble, in *Deformation of Ceramic Materials*, edited by R. C. Bradt and R. W. Tressler (Plenum, New York, 1975), p. 61.
[18] C. Zener, Phys. Rev. **60**, 906 (1941).
[19] T.-S. Kê, Phys. Rev. **71**, 533 (1947).
[20] J. E. Hilliard and J. W. Cahn, Trans. AIME **221**, 344 (1961).
[21] A. S. Nowick and B. S. Berry, *Anelastic Relaxation in Crystalline Solids* (Academic, New York, 1972).
[22] T.-S. Kê, Phys. Rev. **72**, 41 (1947).
[23] A. Salvi, D. Dautreppe, and E. Friess, Rev. Sci. Instrum. **36**, 198 (1965).
[24] G. Pezzotti and K. Ota, Phys. Rev. B **58**, 11 880 (1998).
[25] M. Vaudin, M. Rühle, and S. L. Sass, Acta Metall. **31**, 1106 (1983).
[26] D. Wolf, J. Am. Ceram. Soc. **67**, 1 (1984).
[27] K. T. Aust and J. W. Rutter, in *Recovery and Recrystallization of Metals*, edited by L. Himmel (Interscience, New York, 1962), p. 131.
[28] J. D. Verhoeven, *Fundamentals of Physical Metallurgy* (Wiley, New York, 1975), p. 169.
[29] D. E. Newbury, B. W. Christ, and D. C. Joy, Metall. Trans. A **5**, 1508 (1974).
[30] J. Cho, H. M. Chan, M. P. Harmer, and J. M. Rickman, J. Am. Ceram. Soc. **81**, 3001 (1998).
[31] D. G. Brandon, Acta Metall. **14**, 1479 (1966).
[32] S. Lartigue and L. Priester, J. Phys. C **5-49**, 451 (1988).
[33] D. M. Duffy and P. W. Tasker, Philos. Mag. A **50**, 155 (1984).
[34] C. B. Carter and K. J. Morissey, in *Advances in Ceramics*, edited by W. D. Kingery (The American Ceramic Society, Inc., Columbus, OH, 1984), Vol. 10, p. 303.
[35] W. R. Wagner, T. Y. Tan, and R. W. Balluffi, Philos. Mag. **29**, 895 (1974).
[36] G. Pezzotti, K. Ota, and H.-J. Kleebe, J. Am. Ceram. Soc. **79**, 2237 (1996).
[37] R. Raj and M. F. Ashby, Metall. Trans. A **2A**, 1113 (1971).
[38] D. R. Mosher and R. Raj, Acta Metall. **22**, 1469 (1974).
[39] V. S. Stubican and J. W. Osenbach, in *Advances in Ceramics* (Ref. 34), p. 406.
[40] R. S. Gordon, in *Advances in Ceramics* (Ref. 34), p. 418.
[41] R. M. Cannon, W. H. Rhodes, and A. H. Heuer, J. Am. Ceram. Soc. **63**, 46 (1980).
[42] W. Komatsu and Y. Ikuma, Z. Phys. Chem., Neue Folge **131**, 79 (1982).
[43] P. Feltham, Acta Metall. **5**, 97 (1957).
[44] R. E. Mistler and R. L. Coble, J. Appl. Phys. **45**, 1507 (1974).
[45] Y. Ikuma and W. Komatsu, in *Advances in Ceramics* (Ref. 34), p. 464.
[46] J. Eastman, F. Schmückle, M. D. Vaudin, and S. L. Sass, in *Advances in Ceramics* (Ref. 34), p. 324.
[47] J. M. Vieira and R. J. Brook, in *Advances in Ceramics* (Ref. 34), p. 438.
[48] C. F. Yen and R. L. Coble, J. Am. Ceram. Soc. **55**, 507 (1972).
[49] W. M. Robertson and F. E. Ekstrom, in *Materials Science Research*, edited by T. J. Gray and V. D. Frechette (Plenum, New York, 1969), Vol. 4, p. 271.
[50] T. Maruyama and W. Komatsu, J. Am. Ceram. Soc. **58**, 338 (1975).
[51] W. M. Robertson and R. Chang, in *Materials Science Research*, edited by W. W. Kriegel and H. Palmour, III (Plenum, New York, 1966), Vol. 3, p. 49.
[52] S. Pearson and L. Rotherham, Trans. AIME **206**, 881 (1956).